

A New Iwan / Palmov Implementation for Fast Simulation and System Identification

Drithi Shetty

University of Wisconsin - Madison

ddshetty@wisc.edu

Matthew S. Allen

University of Wisconsin - Madison

msallen@engr.wisc.edu

ABSTRACT

While Iwan elements have been shown to be an effective model for the stiffness and energy dissipation in bolted joints, they are presently somewhat expensive to integrate. Currently, the Newmark-beta algorithm is used to integrate the equations of motion when a structure contains Iwan elements, and a small time step is needed to maintain accuracy. This paper presents a new way of simulating Iwan elements that speeds up the simulations dramatically by using closed form expressions for the micro-slip regime and using an averaging method for regions of time in which no external force is applied. With this method the response can be computed in about a hundredth of the time. The proposed algorithm is demonstrated on a single degree-of-freedom (SDOF) system to understand the range over which it retains accuracy. Although current implementation is applicable to SDOF systems, it can simulate the response of each mode in a structure that is modeled using the modal Iwan approach (i.e. assuming uncoupled, weakly-nonlinear modes).

Keywords: Non-linear damping, Iwan model, method of averaging, Newmark-beta integration, Runge-Kutta

1. Introduction

Built-up structures are typically modeled using linear solvers with springs approximating the joints and using modal or proportional damping to account for energy dissipation. However, mechanical joints are a major contributor to the overall damping of structures [1]. Their behavior is predominantly non-linear and the development of a predictive model for the same is a challenge [2]. At lower amplitudes, only the edges of the joint surfaces slide relative to each other while a majority of the joint remains intact, known as micro-slip. In the micro-slip regime, the stiffness of the joint decreases only slightly, but there is significant energy loss [3]. Hence, the response is nearly linear although the damping is observed to change significantly with the amplitude of vibration [4]. As the amplitude increases, the slip region gradually expands until macro-slip occurs. In this case, relative motion occurs between the surfaces and the stiffness of the joint is significantly affected.

While the physics just described could be captured by modeling each joint in detail with a suitable friction law between parts, to compute the dynamic response with such an approach would take months or years on current computers. As a result, it is more common to use a reduced model with nonlinear elements between each component to account for micro- and macro-slip in the joints. The Iwan element, initially introduced for metal elasto-plasticity [5], has been shown to be effective in capturing joint behavior [4]. It

is a lumped, hysteretic model consisting of a parallel system of spring-slider units known as Jenkins elements. The most common Iwan model is Segalman's four parameter model [6], with the four parameters accounting for the joint stiffness, the force at which the joint slips completely and the power law energy dissipation that many joints have been found to exhibit in microslip. While this is far less computationally expensive than modeling the contact in detail, the computational burden is significant when many joints are present or when performing parameter studies. As an alternative, Segalman proposed a modal approach [8], which exploits the fact that the modes of a structure tend to be mostly uncoupled when the joints remain in the micro-slip regime [9] and hence, each mode can be modeled as a single degree of freedom system but with an Iwan element to account for the nonlinearity.

In either case, the response of a structure that contains Iwan elements is typically found using the average acceleration Newmark-beta integration method [10], with a Newton-Raphson iteration loop for the nonlinear force in the Iwan model. This method is effective and quite reliable, but requires a small time step, making it computationally expensive. This paper presents an alternative that is much less expensive. One study that is relevant to the current work is that on the RIPP joint, presented by Brake in [11], which uses somewhat similar concepts in an effort to accelerate integration of Iwan joints, while preserving the ability of the joint to capture macro-slip.

This work makes use of the analytical formulas for the behavior of an Iwan joint in microslip but limits the solution to the micro-slip regime and uses the averaging method to compute the time response much more quickly. The averaging method is applicable to systems in which the amplitude and phase vary slowly with time [12]. The following integration technique takes advantage of this behavior to improve the simulation time without significantly affecting the accuracy. It also has the advantage that the instantaneous natural frequency and damping are computed in the course of the time integration. The subsequent section explains the algorithm and the relevant theory behind it. Its applicability for a single degree of freedom system is then examined through a case study and future research is proposed.

2. Understanding the algorithm

The algorithm presented in this work considers a single degree of freedom system (shown in Figure 1) consisting of a linear spring, linear damper and a single non-linear Iwan joint. The simulation is divided into two parts –

- Integration in the presence of an external impulsive force and
- Simulating the free decay response after the external force goes to zero.

Matlab's adaptive 4th-5th order Runge-Kutta (RK) algorithm (i.e. ode45), is used for both parts. This requires that the differential equation be defined in the form $\dot{\mathbf{x}} = f(\mathbf{x}, t)$ with the initial conditions provided as input. It is important to note that the traditional Iwan element cannot be integrated using Runge-Kutta, because it is hysteretic by definition and so it cannot be written in the form described above (without some kind of approximation). For that reason, the Newmark-beta algorithm has been used with a fixed time step in most cases in the literature. The procedure for obtaining the initial conditions is explained below.

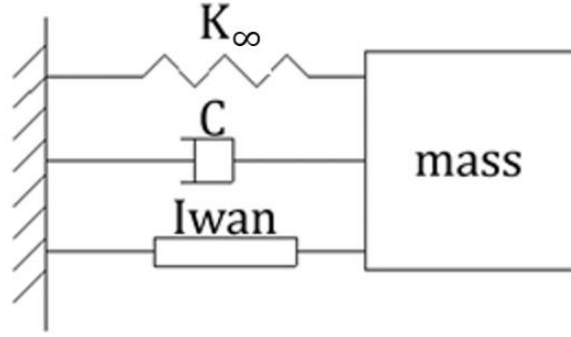


Figure 1: Schematic of the single degree of freedom system

2.1 When the external force is non-zero

The forced equation of motion can be approximated as follows when the Iwan joint remains in the micro-slip regime,

$$\ddot{x} + 2\zeta(A)\omega_n(A)\dot{x} + (\omega_n(A))^2x = F(t)/m \quad (1)$$

where A is the amplitude of vibration, which is elaborated below. The closed form expressions of dissipation per cycle (D) and secant stiffness (K_j) derived in [6] are used after converting the physical Iwan parameters [F_s, K_t, χ, β] to their mathematical equivalents [R, S, χ, ϕ_{max}]

$$D = \frac{4RA\chi^3}{(\chi + 3)(\chi + 2)} \quad (2)$$

$$r = \frac{A}{\phi_{max}} \quad (3)$$

$$K_j = K_t \left(1 - \frac{r^{\chi+1}}{(\chi + 2)(\beta + 1)} \right) \quad (4)$$

Equations 2, 3 and 4 are then substituted in the expressions below to obtain the effective natural frequency and damping ratio.

$$\omega_n(A) = \frac{\sqrt{K_j(A) + K_\infty}}{m} \quad (5)$$

$$\zeta(A) = \frac{D(A)}{2\pi m \omega_n^2 A^2} + \zeta_{linear} \quad (6)$$

By assuming that the change in amplitude is negligible over each cycle, a relationship between amplitude and response can be established as shown in equations 7 through 9,

$$x \cong A \cos(\omega_d t) \quad (7)$$

$$\dot{x} \cong -A \omega_d \sin(\omega_d t) \quad (8)$$

$$A = \sqrt{x^2 + \left(\frac{\dot{x}}{\omega_d} \right)^2} \quad (9)$$

where

$$\omega_d = \omega_n \sqrt{1 - \zeta^2} \quad (10)$$

As seen in the equations above, the amplitude, natural frequency and damping ratio are interdependent variables in that the amplitude also changes with changing ω_n and ζ . This makes it necessary to solve this iteratively. To do so, a simple recursive scheme is implemented. The amplitude (and corresponding ω_n and ζ) is calculated within a loop, and the loop is repeated until the absolute difference between the amplitude calculated in successive iterations falls within a pre-defined tolerance. It was observed that a reduction in tolerance below 10^{-10} led to negligible change in the simulated response. Three to four loop iterations were typically needed. The instantaneous natural frequency and damping ratio thus obtained are then substituted in the equation of motion which is used to define the ODE that is solved.

The solution at the time at which the force ends (i.e. assuming the force is impulsive or otherwise short in duration) is used to define the initial amplitude and phase of the solution for the averaging algorithm, which solves for the rest of the transient response and is described in the next subsection.

2.2 When the external force is zero

The equation of motion in the absence of external force becomes the following.

$$\ddot{x} + 2\zeta(A)\omega_n(A)\dot{x} + (\omega_n(A))^2x = 0 \quad (11)$$

While the previous method could be used for the transient part of the response as well, a quicker solution can be achieved by using the averaging method. On analyzing the response, it can be seen that while the response itself changes quickly with time, the amplitude and phase of the response change slowly with time (as seen in figure 2). Under these circumstances, the averaging method can be used to change the variables in the differential equation from displacement and velocity to amplitude and phase, allowing larger time steps to be taken and thus achieving a less computationally expensive solution. The differential equations used in this algorithm are derived in [13] by replacing displacement and velocity as states with amplitude and phase and then integrating over a cycle (i.e. assuming that amplitude and phase change slowly with time). The result is given in equations 12 and 13.

$$\dot{A} = -A\omega_n\zeta \quad (12)$$

$$\dot{\phi} = \omega_n\sqrt{(1 - \zeta^2)} \quad (13)$$

As given in the derivation in [13], once these are found as a function of time, the displacement and velocity can then be recovered (if desired), using the following.

$$x = Ae^{i\phi} \quad (14)$$

$$\dot{x} = \dot{A}e^{i\phi} + A\dot{\phi}e^{i\phi}i \quad (15)$$

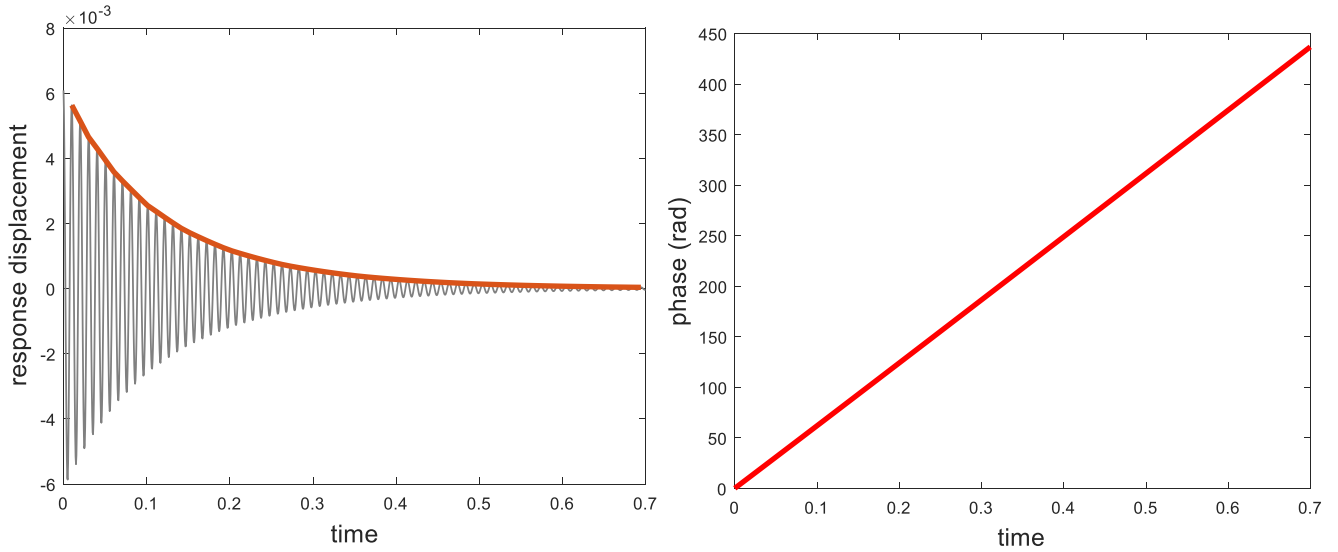


Figure 2: Response amplitude and phase vs time

3. Application to single degree of freedom system

The algorithm described was tested against the Newmark-beta integration technique for speed and accuracy. The accuracy was measured by quantifying the error in the effective damping ratio and natural frequency as a function of amplitude and the speed was measured as the time taken for integration on an Intel® Core™ i7-950 (3.07 GHz) processor. The response displacement (and velocity) were simulated using three methods:

- Newmark-beta integration
- The algorithm described in Sec. 2.1 and 2.2, which is referred to here simply as the “Averaging” algorithm
- A combination of the Newmark-beta algorithm (replacing the algorithm in Sec. 2.1) with the averaging algorithm of Sec. 2.2, which is here referred to as “NB+Averaging”

Table 1: Parameters used in the test case

Parameter	Value
K_{∞}	$1.4 \times 10^5 \text{ N/m}$
ζ_{linear}	1×10^{-4}
Iwan Joint:	
• $[F_s, K_t, \chi, \beta]$	$[40000 \text{ N}, 2.5 \times 10^5 \text{ N/m}, -0.5, 1.0]$
Half sinusoidal pulse:	
• Amplitude	(varies)
• Pulse-width	0.02 s

Table 1 lists the parameters defining the test case being considered. A half sinusoidal impulse force of width 0.02s was applied at various amplitudes, focusing on the micro-slip regime. This was verified by checking the displacement of the sliders in the Iwan joint. The time responses obtained by each method were then processed using the Hilbert transform, as described in [14], to obtain the instantaneous

damping ratio and natural frequency. The errors in these estimations were calculated treating the Newmark-beta result as the truth solution, although some difficulty was encountered when doing this, as explained in the subsequent section.

3.1 Results and Analysis

3.1.1 Accuracy

Figure 3 shows a sample of the responses obtained from the three simulation methods, corresponding to the case where the force amplitude was 10 kN, (or $E_r = 0.9$, as will be defined subsequently). The response was found for 40 seconds in each case. Then, the Hilbert transform was computed and trimmed to mitigate the end effects, as shown in Figure 4. To maintain consistency, the same trim points were used for all simulation methods. The damping ratio and natural frequency obtained from the Hilbert transform were then plotted against the response velocity amplitude to observe the power-law behavior. It must be noted here that these graphs progress from right to left (i.e. from higher velocity amplitudes to lower velocity amplitudes) since the response velocity decreases with time. To generalize the results, the non-dimensional velocity was defined as the ratio of the velocity to the product $(\omega_{n,0} \phi_{max})$, where $\omega_{n,0}$ is the natural frequency when the joint is stuck and ϕ_{max} , the displacement of the joint at macro-slip. The error in damping ratio and natural frequency was then calculated as a percentage of the Newmark-beta solution, which was considered to be the truth solution.

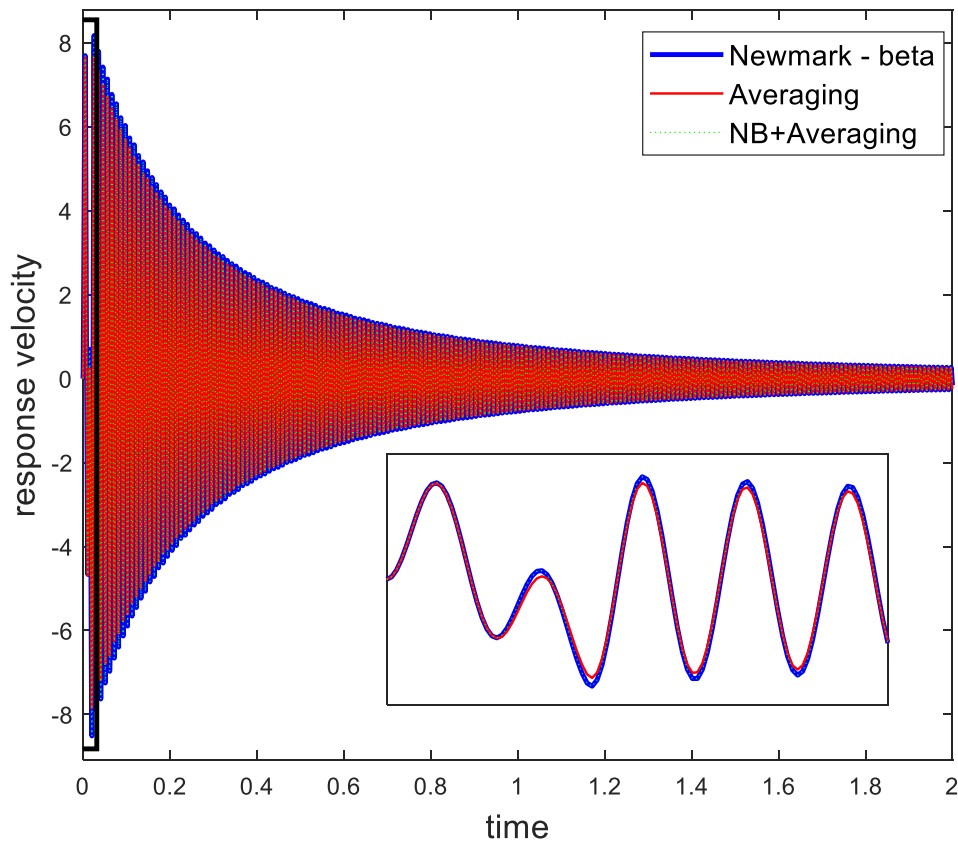


Figure 3: Response velocity predicted by the three methods

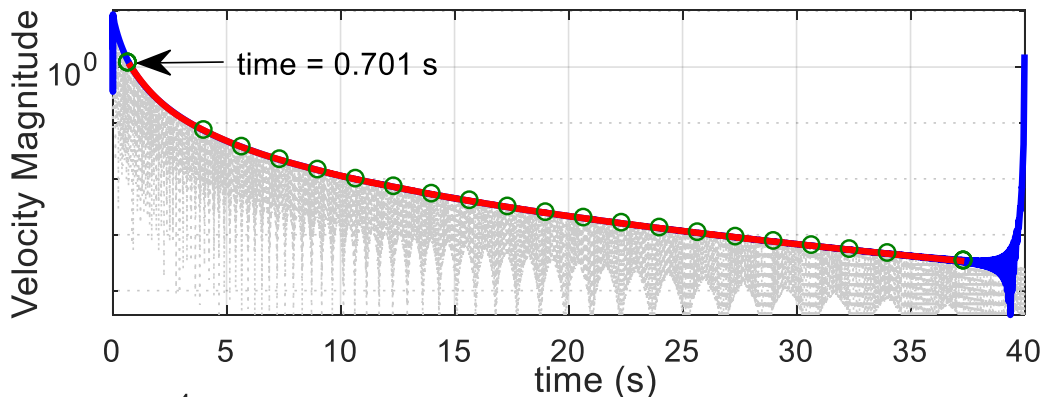


Figure 4: Trimming the velocity vector after computing the Hilbert transform to eliminate end effects

On performing the simulation for the test case described above, it was initially observed that the damping ratio (and natural frequency) estimated using the derived algorithm deviated from that obtained using the Newmark-beta (NB) integration at low velocities. As seen in figure 555, the damping ratio calculated by the NB method decreases to values below linear damping at lower velocities. On further investigation, it was noted that the response simulated by the NB method was sensitive to the residual tolerance criterion set in the Newton-Raphson Iteration loop. This was surprising, because the tolerance of 10^{-13} had been used in many previous studies without difficulty, and it was already approaching machine precision. The tolerance was reduced gradually until further reduction did not have a significant effect on the output. Finally, a tolerance of 10^{-15} was found suitable for the range of forces analyzed in this work. The arbitrary nature of this selection highlights a possible drawback of the existing integration method and further warrants development of a more accurate technique.

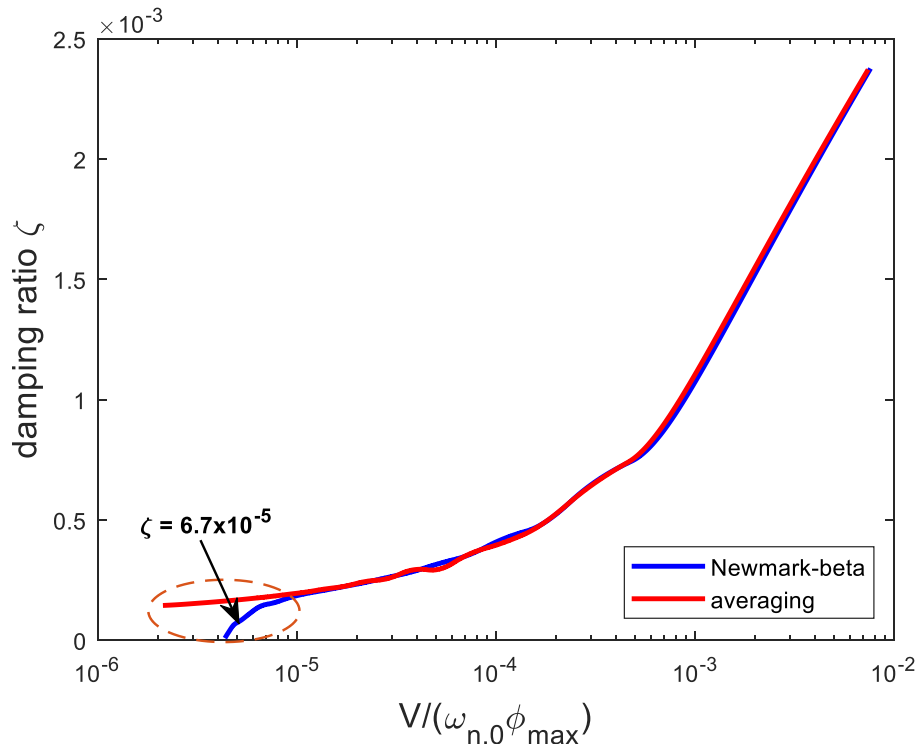


Figure 5: Damping ratio vs non-dimensional velocity when residual tolerance = 10^{-8}

Figure 6 compares the damping ratio and natural frequency calculated by each of the methods after changing the tolerance described above. It can be observed that the results obtained are now in good

agreement with the truth solution. The averaging method is found to give quite accurate results over a large range of vibration amplitude, with errors of less than 0.04% in the natural frequency over the whole range of amplitude and errors in damping of less than 8% (of the true value, which ranged from $\zeta = 0.0001 - 0.003$). The error is most pronounced at a non-dimensional velocity of 10^{-4} , which is possibly due to the noise introduced in the predictions by the Hilbert transform process. As expected, when the averaging method is augmented by using the NB algorithm to compute the initial portion of the response (during which the force is active), the error decreases relative to using the RK integration for initial portion. Note that the first instant shown in Fig. 6 (highest amplitude) corresponds to 0.70 seconds whereas the force pulse lasts 0.02 seconds.

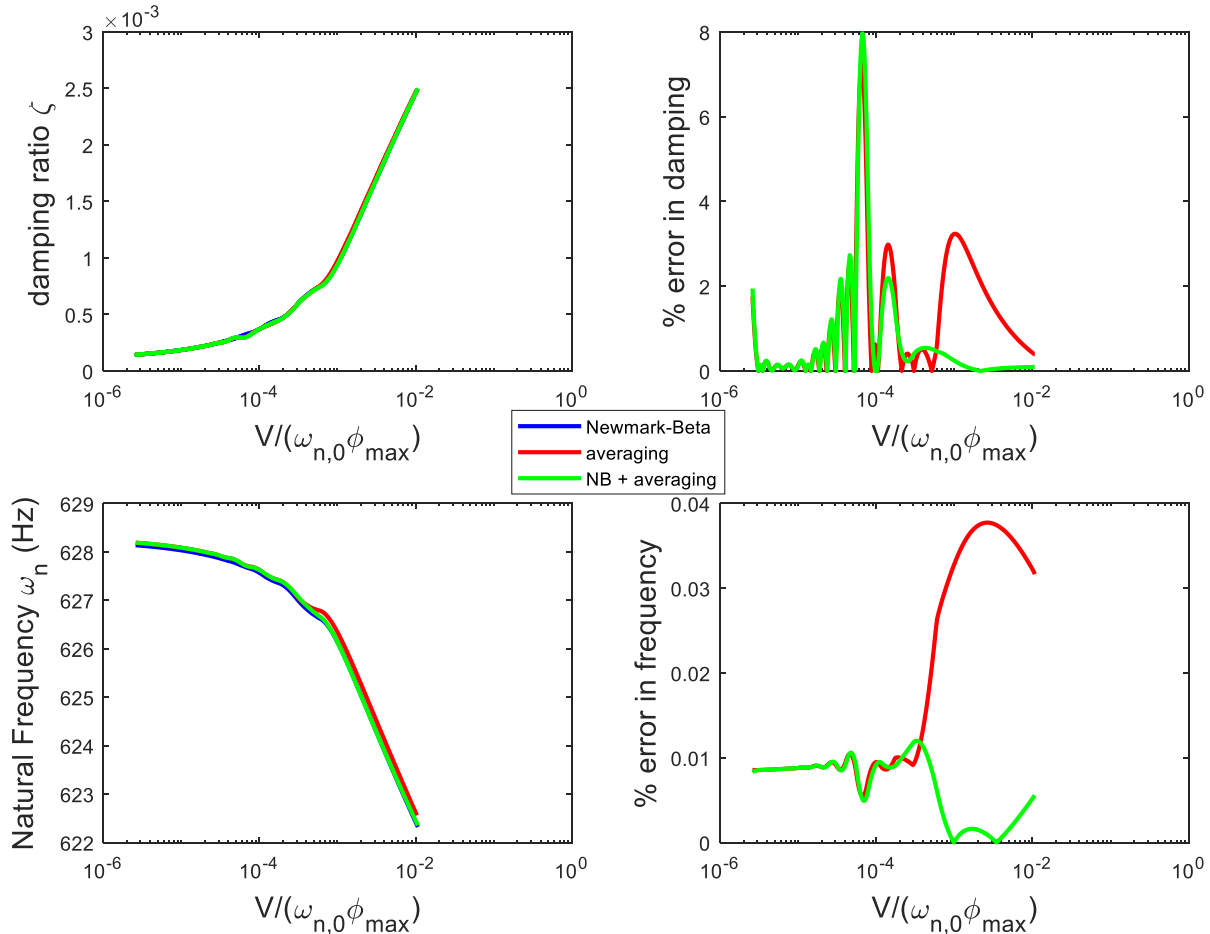


Figure 6: Damping ratio and natural frequency vs non-dimensional velocity

The above plots used the Hilbert transform, which is susceptible to noise and end effects, to estimate the damping ratio and natural frequency from time histories. The Averaging method, however, also estimates the same during the course of the integration (i.e. equations 5 and 6). To evaluate the potential errors in the damping and frequency due to the Hilbert transform, Figure 7 compares the damping estimated directly from the algorithm with those obtained from the Hilbert transform from the NB method and the Averaging method. All three solutions agree very well for non-dimensional velocities below $5 \cdot 10^{-5}$, but the values calculated directly using the Averaging method deviate from those estimated using the Hilbert transform at higher velocities. The damping found by the Hilbert Transform shows a slight waviness that is not expected from theory, whereas the damping found directly by the Averaging method shows exactly the expected power law behavior (i.e. the damping is linear on a log-log plot). Another advantage of the averaging method is that one does not need to truncate the first 0.70 seconds of data, as is required in the Hilbert transform to minimize end effects.

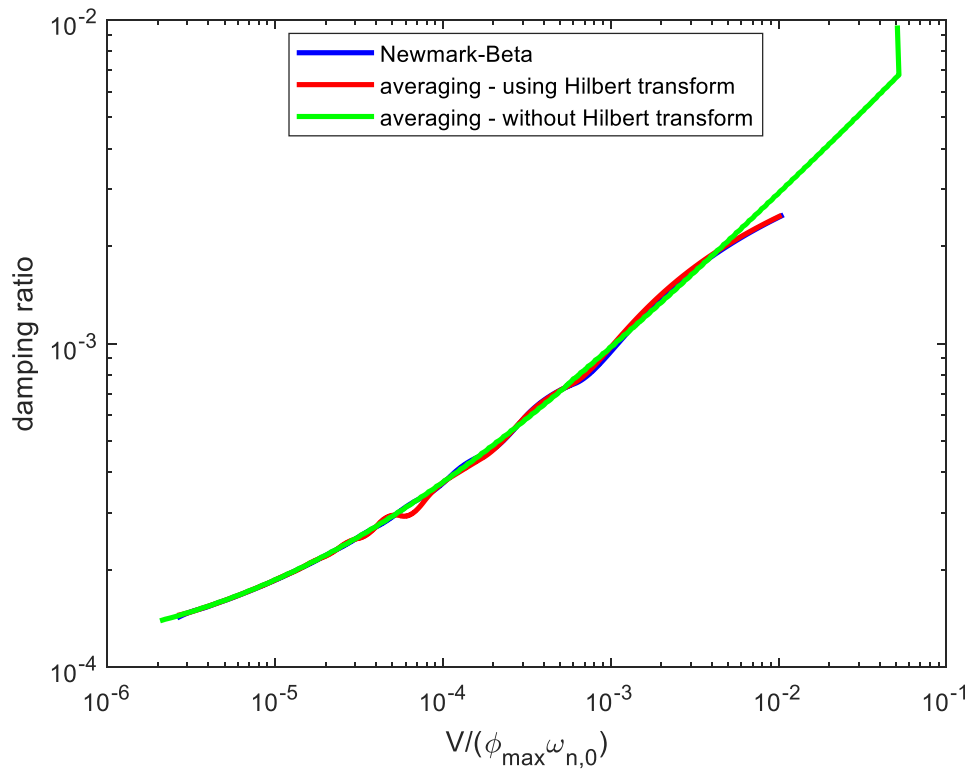


Figure 7: Damping ratio calculated using closed form expressions

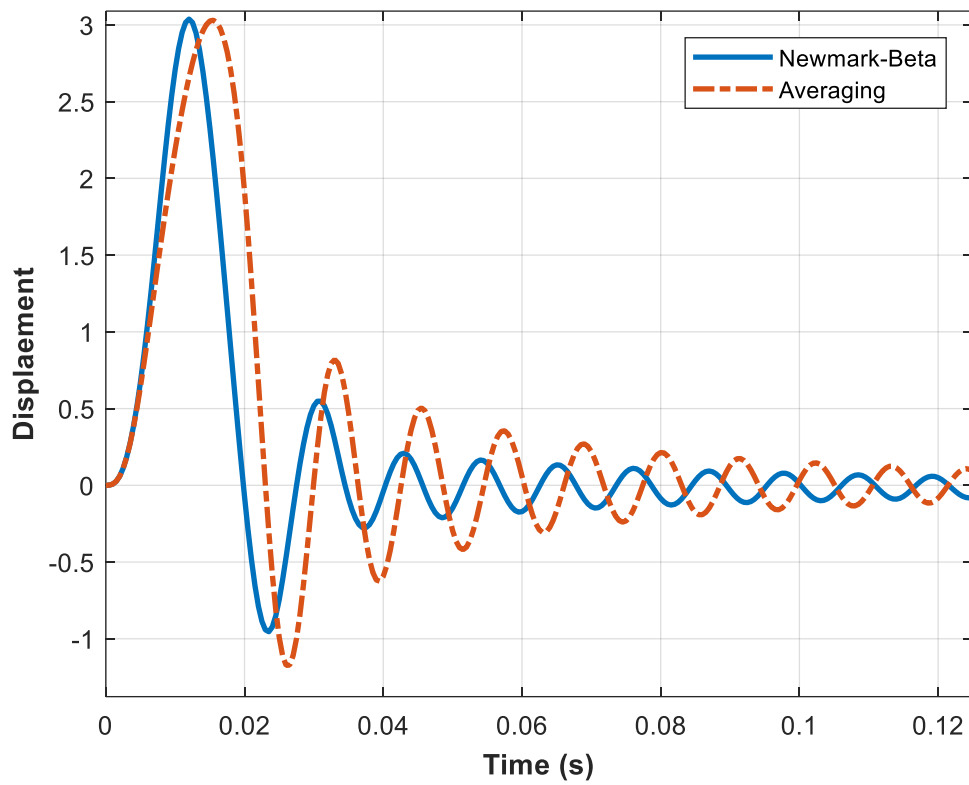


Figure 8: Response velocity vs time, macro-slip

While the results above clearly show that the Averaging method produces a transient response that closely follows the desired frequency versus amplitude and damping versus amplitude curves, they do not prove that the same transient response will be obtained by each algorithm. Specifically, when the joint approaches macro-slip the initial response may deviate significantly, causing the averaging solution to estimate inaccurate amplitudes in the initial phase. An example of this is shown in Figure 8, for the case where the force amplitude was $3 \cdot 10^5$ N (or $E_r = 685$). The averaging method behaves differently over the 0.02 second force pulse, resulting in a higher velocity during the transient part of the response.

To further quantify this, the amplitude of the response was estimated from each method for various force amplitudes and the results are summarized in Figure 9. To generalize the results, the non-dimensional force amplitude was expressed as an energy ratio $E_r = E_{imp}/PE_{max}$ where the numerator is the energy imparted by the impulse (equation 16) and the denominator is the approximate potential energy for which the joint fully slips (equation 17). The results show that the averaging method predicts the transient response amplitude well up until an energy ratio of unity, and still produces acceptable results up until a ratio of 10. Beyond that point, it begins to significantly under-estimate the response amplitude, presumably because it doesn't have the ability to account for macro-slip.

$$E_{imp} = \frac{1}{2m} (\int f(t)dt)^2 \quad (16)$$

$$PE_{max} = \frac{1}{2} (K_{\infty} + K_T) \phi_{max}^2 \quad (17)$$

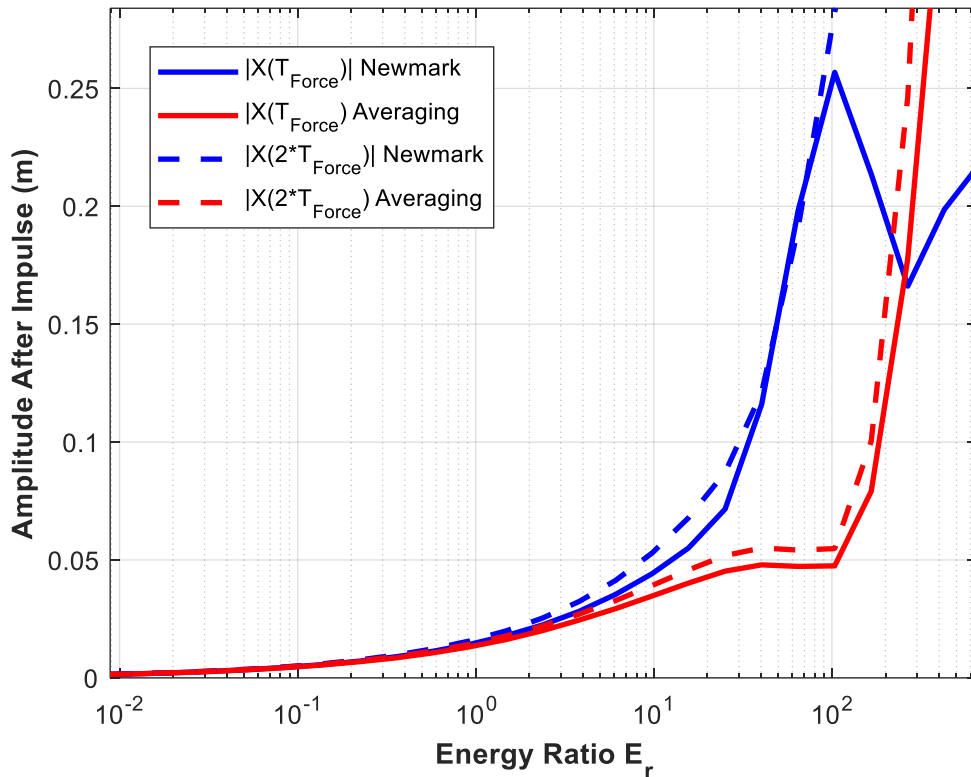


Figure 9: Response amplitude after the impulse has ended for Newmark-beta method and Averaging method. The horizontal axis expresses the force in terms of the energy relative to that which initiates macro-slip, as described above.

3.1.2 Speed

Table 2: Average Simulation time for each of the three methods

Integration Method	Simulation time (in seconds)
Newmark-beta	214.24
Averaging	1.961
Newmark beta and averaging combined (NB+Averaging)	14.303

As a measure of speed, the average simulation time was compared for the range of force amplitudes considered. Table 2 shows the time taken by each of the three methods being compared to simulate the response. It is evident that the method of averaging speeds up the integration process significantly. This was anticipated as applying the concept of averaging allows for a larger time step to be considered, thus lowering the number of integration steps. For example, for the cases shown in figure 10, 79976 time steps were required for the NB method (200 samples per period) whereas for the same duration of interest, with the method of averaging, the RK integrator used an average of 2984 time steps. It can also be observed that varying the amplitude of the impulse force applied does not result in a considerable change in simulation time (Figure 11).

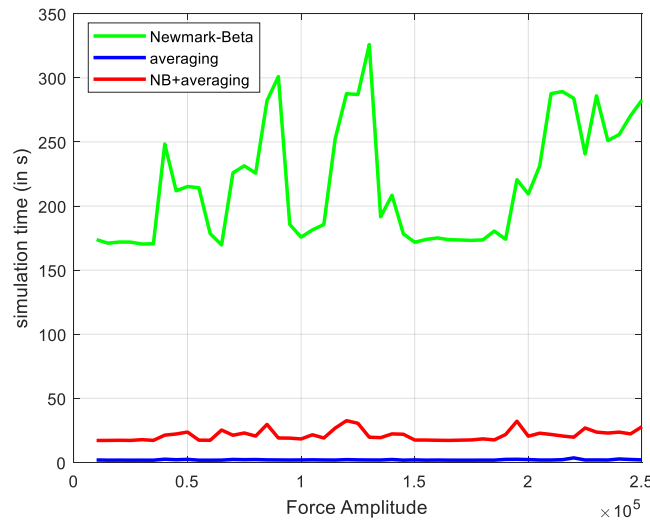


Figure 10: Variation of simulation time with input force amplitude

4. Conclusions

This work has shown that the method of averaging can be effectively used to speed up the integration of a single degree of freedom system with an Iwan joint with minimal loss in accuracy up to surprisingly large forces. In the micro-slip regime, the damping ratio, natural frequency and response amplitude estimated were found to be comparable to those from the Newmark-beta method. In fact, in some cases the averaging method was more reliable and accurate (i.e. didn't require adjusting the ad-hoc convergence tolerance in the Newton loop). It is also preferable if the final goal is to estimate damping and frequency versus time, because no further processing (i.e. with the Hilbert transform) is required to obtain these.

However, the averaging algorithm is fundamentally limited to micro-slip only. One can obtain the best of both worlds by using the Newmark-beta method until the external force dies down and the method of

averaging can be used thereafter. With this approach the computation time is reduced significantly, but not as much so as when only the averaging method is used (i.e. the computation time is only reduced by a factor of ~10 rather than a factor of ~100).

Future work will seek to couple this with a suitable optimization tool, allowing one to determine the modal Iwan parameters for a weakly non-linear mode using frequency domain data. Such an approach could be critical in cases in which modal filtering or bandpass filtering is not applicable.

References

- [1] L. Gaul and J. Lenz, "Nonlinear dynamics of structures assembled by bolted joints," *Acta Mech.*, vol. 125, no. 1, pp. 169–181, Mar. 1997.
- [2] M. R. W. Brake, *The mechanics of jointed structures*. New York, NY: Springer Science+Business Media, 2017.
- [3] D. J. Segalman, "An Initial Overview of Iwan Modeling for Mechanical Joints," SAND2001-0811, 780307, Mar. 2001.
- [4] D. J. Segalman, "Modelling joint friction in structural dynamics," *Struct. Control Health Monit.*, vol. 13, no. 1, pp. 430–453, Jan. 2006.
- [5] W. D. Iwan, "A Distributed-Element Model for Hysteresis and Its Steady-State Dynamic Response," *J. Appl. Mech.*, vol. 33, no. 4, pp. 893–900, Dec. 1966.
- [6] D. J. Segalman, "A Four-Parameter Iwan Model for Lap-Type Joints," p. 55.
- [7] D. Segalman and W. Holzmann, "Nonlinear response of a lap-type joint using a whole-interface model," Jan. 2005.
- [8] D. J. Segalman, "A modal approach to modeling spatially distributed vibration energy dissipation.," SAND2010-4763, 993326, Aug. 2010.
- [9] B. J. Deaner, M. S. Allen, M. J. Starr, and D. J. Segalman, "Investigation of Modal Iwan Models for Structures with Bolted Joints," in *Topics in Experimental Dynamic Substructuring, Volume 2*, 2014, pp. 9–25.
- [10] R. D. Cook, D. S. Malkus, M. E. Plesha, and R. J. Witt, *Concepts and applications of finite element analysis*, vol. 4. Wiley New York, 1974.
- [11] M. R. W. Brake, "A reduced Iwan model that includes pinning for bolted joint mechanics," *Nonlinear Dyn.*, vol. 87, no. 2, pp. 1335–1349, Jan. 2017.
- [12] A. H. Nayfeh, *Introduction to Perturbation Techniques*, 1 edition. New York: Wiley-VCH, 1993.
- [13] A. H. Haslam *et al.*, "Non-linear system identification in the presence of modal coupling," p. 20.
- [14] A. Sumali, "Calculating Damping from Ring-Down Using Hilbert Transform and Curve Fitting," p. 20.